Rapid Fabrication of Two- and Three-Dimensional Colloidal Crystal Films via Confined Convective Assembly

ARTICLE *in* ADVANCED FUNCTIONAL MATERIALS · AUGUST 2005

Impact Factor: 11.81 · DOI: 10.1002/adfm.200400602

3 AUTHORS, INCLUDING:

Mun Ho Kim
Korea Research Institute of Chemical Tech…
36 PUBLICATIONS **933** CITATIONS
SEE PROFILE

Sang Hyuk Im
Kyung Hee University
199 PUBLICATIONS **9,202** CITATIONS
SEE PROFILE

ADVANCED FUNCTIONAL MATERIALS

Rapid Fabrication of Two- and Three-Dimensional Colloidal Crystal Films via Confined Convective Assembly**

By *Mun Ho Kim*, *Sang Hyuk Im*, and *O Ok Park**

We have developed a self-assembly method for fabricating well-ordered two-dimensional (2D) and three-dimensional (3D) colloidal crystal films. With a minute amount of a polystyrene colloidal suspension and without any special equipment, the proposed method can be used to rapidly deposit high-quality colloidal crystal films over a large surface area. By controlling the lift-up rate of the substrate, we modulate the meniscus thinning rate, which determines whether the colloidal particles are assembled into two or three dimensions. The proposed method can be used to fabricate not only monolayered colloidal crystals with colloidal particles of various sizes, but also multilayered colloidal crystals. In addition, the method enables us to fabricate binary colloidal crystals by consecutively depositing large and small particles.

1. Introduction

Because of potential applications, the assembly of submicrometer-sized colloidal particles into ordered two-dimensional (2D) and three-dimensional (3D) structures, called colloidal crystals, has been intensively studied over the past decade. 2D colloidal crystals have been achieved with good reproducibility using techniques such as spin-coating,[1] deposition with lateral capillary force,[2] and Langmuir–Blodgett (LB)[3] and electrophoretic deposition.[4] 2D colloidal crystals can be used as masks for photolithography,[5] templates for the epitaxial growth of colloidal particles,[6] and master molds for 2D regular arrays. Recently, 3D colloidal crystals have attracted a great deal of attention because of their unique structure and optical properties. They could, for instance, be employed as photonic bandgap materials that can manipulate the propagation of light.[7] These crystals have potential use in various applications such as templates for macroporous materials or inverse opals,[8] waveguides,[9] switches,[10] and optical filters,[11] as well as in chemical and biochemical sensors.[12] Typical methods for 3D colloidal assembly are gravitational sedimentation,[13] vertical deposition,[14] vertical deposition with a temperature gradient,[15] electrophoresis,[16] colloidal assembly at an air–water interface,[17] and isothermal heating evaporation-induced self-assembly (IHEISA).[18]

We describe a new procedure, termed confined convective assembly, which can be used to produce well-ordered 2D and 3D colloidal crystal films in a single step. This new method has several advantages over previously reported procedures. First, 2D or 3D colloidal crystals can be deposited rapidly using colloidal particles of various sizes over large areas with very small quantities of a polystyrene (PS) colloidal suspension. Without any special equipment, it can be used to produce well-ordered 2D or 3D colloidal crystals over large areas (1 cm × 1 cm) in several minutes. In addition, it is inexpensive because it uses only minute quantities of the PS colloidal suspension (100 μL at one time).

Second, when we fabricate colloidal multilayers with our method, we can control the thickness at the layer level. Controlling the thickness of colloidal crystals is important because the thickness is related to their optical properties. Our method enables us to elaborately control the thickness of the colloidal crystals by controlling the experimental factors (the lift-up rate of the substrate and the concentration of the colloidal suspension). Moreover, we can fabricate colloidal multilayers by consecutively deposing the colloidal particles; that is, with layer-by-layer growth.

Third, we can easily produce binary colloidal crystals by consecutively depositing layers of large and small colloidal particles. Binary colloidal crystals have not yet been extensively investigated as single-component colloidal crystals because they are harder to grow and characterize.[19] We now discuss in detail the fundamentals of our method, along with the experimental considerations and results.

2. Results and Discussion

When a colloidal suspension, e.g., one in a water medium, is dropped onto a wettable substrate, such as a glass or silicon wafer, the colloidal particles in the suspension move towards the edge of the colloidal droplet. This phenomenon occurs because the water evaporation rate is highest at the edge of the suspension droplet, which causes a water influx toward the edge

[*] Prof. O O. Park, M. H. Kim, Dr. S. H. Im[+]
Department of Chemical and Biomolecular Engineering
Korea Advanced Institute of Science and Technology
373-1 Guseong-dong, Yuseong-gu, Daejeon 305-701 (Korea)
E-mail: ookpark@kaist.ac.kr

[+] Present address: LG Chem. Ltd., Research Park, 104-1 Moonji-dong, Yuseong-gu, Daejeon 305-380, Korea.

[**] The authors are grateful to the Center for Advanced Functional Polymers, which is supported by KOSEF. This work was partially supported by the Brain Korea 21 Project of the Korean Ministry of Education and Human Resources. Supporting Information is available online form Wiley InterScience or from the author.

 DOI: 10.1002/adfm.200400602

(Fig. 1a).[20] The water influx transports the colloidal particles toward the edge and they assemble into ordered structures because of the lateral capillary force (Fig. 1c). In addition, as the assembled colloidal particles are pinned at the edge, they form a contact line (Fig. 1b). The pinned colloidal particles fix the contact line and cause further water influx toward the edge. Accordingly, the colloidal particles continuously move towards the fixed boundary (contact line) and assemble three-dimensionally.

To exploit these pinning and assembling phenomena, we devised the experimental set-up depicted in Figure 2a. (Fig. S1, Supporting Information, gives photographs of the experimental set-up for confined convective assembly.) First, we connected a glass substrate (the back glass substrate) to a dipping machine to control the lift-up rate. We then attached a front glass substrate that was separated from the back glass substrate by a gap of approximately 100 μm. We inserted the colloidal suspension (about 100 μL) into the gap with a capillary force that was large enough to sustain the colloidal suspension in the gap. Finally, we raised the back glass substrate at a specific rate while blowing hot air towards the meniscus that formed at the interface of the glass substrate and the colloidal suspension. The hot air was blown towards the meniscus in order to evaporate the water in the colloidal suspension; water evaporation not only assembles the colloidal particles into ordered structures but also fixes them onto the back glass substrate. The water evaporation also generates water influx toward the meniscus edge (that is, the edge of the contact line).

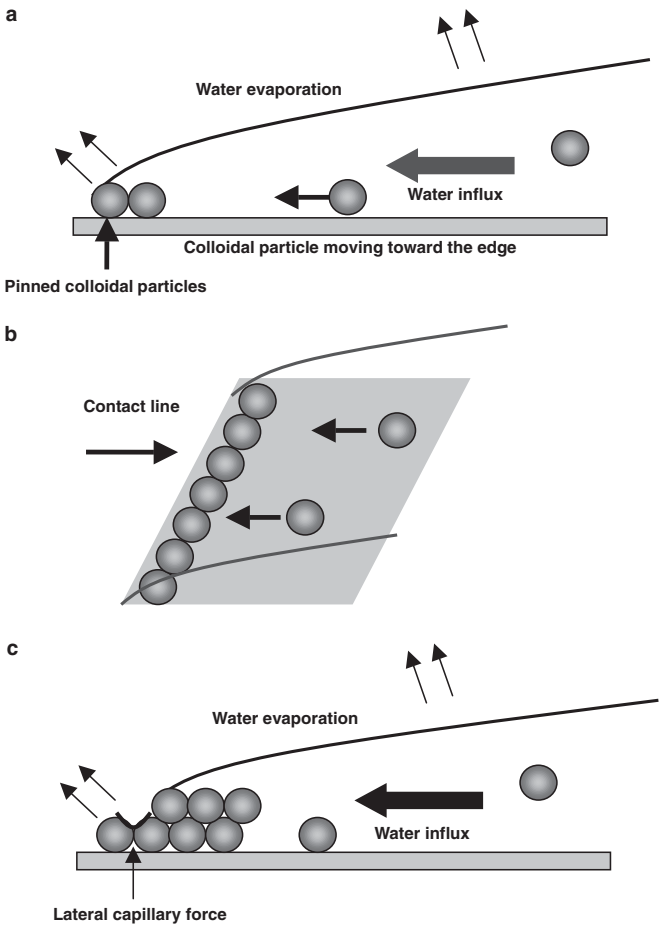

Figure 1. Schematic illustration of colloidal particles assembling at the meniscus of a colloidal suspension droplet. In the early stage, the colloidal particles assemble into a monolayer: a) side view of the monolayer and b) top view of the monolayer. As time elapses, colloidal particles assemble into a multilayer: c) side view of the multilayer.

To fabricate 2D colloidal crystals with this procedure, we used a 0.5 wt.-% PS (colloids 460 nm in diameter) colloidal suspension (water medium). The colloidal particles should assemble into a monolayer at the meniscus (the interface between the back glass substrate and the colloidal suspension) to be ordered two-dimensionally on the back glass substrate. The shape of the meniscus determines whether the colloidal particles assemble into a mono- or a multilayer.[21] If the shape of the meniscus is steep, the colloidal particles assemble into a monolayer; if not, they assemble into a multilayer. The shape of the meniscus is controlled by the rate at which the back glass substrate is lifted (Fig. 2b). Thus, the colloidal crystal structure that is generated (the monolayer or the multilayer) can be controlled by the lift-up rate at a fixed concentration. This control is possible because the colloidal particles pinned at the meniscus edge fix the contact line. We examined how the colloidal particles assemble on the glass substrate for various lift-up rates (Figs. 2b–e).

When the lift-up rate was 20 $\mu m\,s^{-1}$, the colloidal crystals were found to assemble into a multilayer. Under these experimental conditions, the lift-up rate is too slow to cause the colloidal particles to assemble into a monolayer at the meniscus, because, at this lift-up rate, a smooth meniscus is formed. As depicted in Figure 2c, a smooth meniscus provides colloidal particles with enough space to assemble into a multilayered structure. Figure 3a shows the surface image obtained via scanning electron microscopy (SEM). The image shows that another layer exists under the top layer, which provides conclusive evidence that, under these conditions, the colloidal particles assemble into a multilayer. (To be exact, the multilayer is a trilayer as shown in Figure 3b, and we also obtained a bilayer, obtained at a lift-up rate of 30 $\mu m\,s^{-1}$.) Thus, multilayered colloidal crystals can be obtained with this fabrication method, in which the thickness of the colloidal crystal is determined by the meniscus thinning rate, that is, by the lift-up rate.

At a lift-up rate of 45 $\mu m\,s^{-1}$, the colloidal particles assemble into a monolayer. In this case, the lifting of the glass substrate results in a meniscus that is sufficiently steep to facilitate the assembly of the colloidal particles into a monolayer (Fig. 2d). Figure 3c present the resulting SEM surface image, which clearly shows that the colloidal particles have assembled into a monolayer. (Fig. S2, Supporting Information, shows a photograph of the sample obtained at the lift-up rate of 45 $\mu m\,s^{-1}$.) The sample shows the iridescent color that typically appears in ordered colloidal crystals. The photograph (Fig. S2) also shows that the colloidal particles are highly ordered over a large area.

Last, at a lift-up rate of 75 $\mu m\,s^{-1}$, colloidal particles assemble into sparse structures (Fig. 3d). These structures appear because the lift-up rate is too fast, so the colloidal particles have

ADVANCED FUNCTIONAL MATERIALS

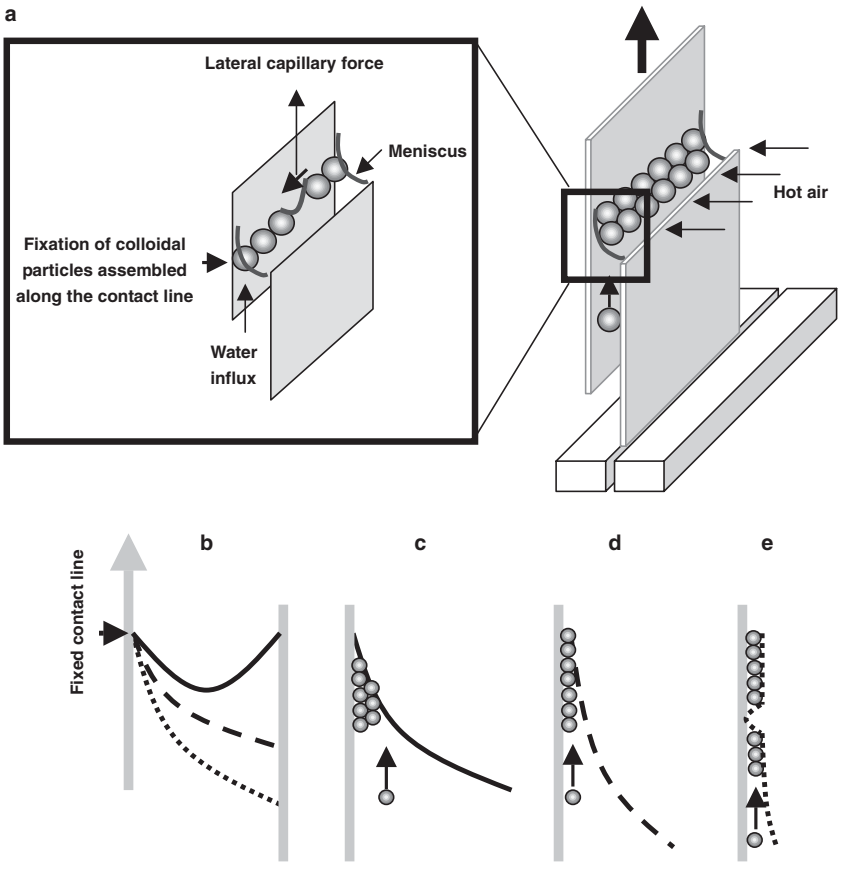

Figure 2. a) The experimental set-up. The magnified image schematically shows the phenomena that occur at the meniscus. b) The shape of the meniscus as it varies with lift-up rates of c) 20 $\mu m\,s^{-1}$, d) 45 $\mu m\,s^{-1}$, and e) 75 $\mu m\,s^{-1}$.

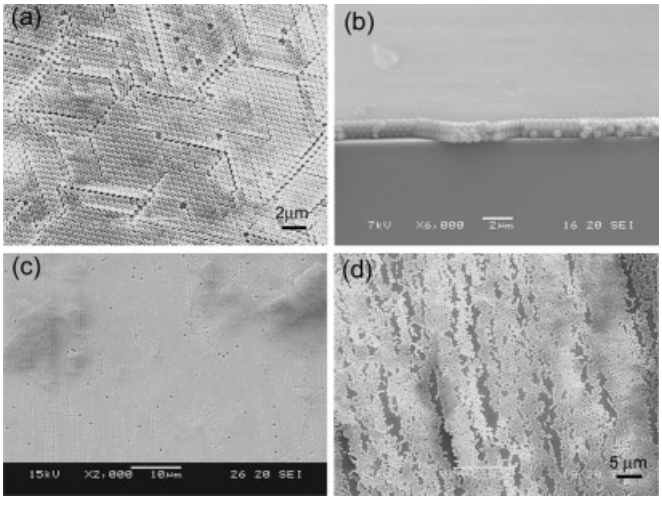

Figure 3. SEM surface images of colloidal crystals with a lift-up rate of a) 20 $\mu m\,s^{-1}$, b) side view of the trilayer. SEM surface images of colloidal crystals with lift-up rates of c) 45 $\mu m\,s^{-1}$ and d) 75 $\mu m\,s^{-1}$.

insufficient time to move up to the edge of the contact line (Fig. 2e). Hence, the colloidal particles are deposited onto the glass substrate before reaching the ordered region (contact-line edge) owing to the steep meniscus shape.

To obtain monolayered colloidal crystals over a large area, we therefore need an appropriate lift-up rate (here 45 $\mu m\,s^{-1}$). Furthermore, the appropriate lift-up rate for fabricating monolayered colloidal crystals increases with the concentration of the colloidal suspension. When the concentration is higher than 0.5 wt.-%, we need to lift the substrate faster than 45 $\mu m\,s^{-1}$ in order to fabricate the monolayer, and vice versa. The appropriate lift-up rate was 55 $\mu m\,s^{-1}$ for a 0.7 wt.-% PS colloidal suspension and 25 $\mu m\,s^{-1}$ for a 0.3 wt.-% PS colloidal suspension.

The thickness of the assembled colloidal crystal depends on the meniscus thinning rate and the velocity of colloidal particles moving towards the contact line. Hence, the thickness of the colloidal crystal can be controlled by the lift-up rate, the concentration of the colloidal suspension, and the evaporation rate of water. We have shown that the thickness of the colloidal crystals can be controlled by varying the lift-up rate. We then tried to fabricate multilayered colloidal crystals by changing the concentration of the colloidal suspension. In this experiment, we used 1.0 wt.-% and 2.0 wt.-% PS colloidal suspensions (PS colloid 460 nm in diameter), and we lifted the back glass substrate at a rate of 45 $\mu m\,s^{-1}$. When the concentration of the colloidal suspension was 1.0 wt.-%, the resulting colloidal crystals formed a bilayer. In addition, when the concentration of the colloidal suspension is 2.0 wt.-%, a tetralayer is obtained. Figures 4a,b show the side-view SEM images of each sample. When we increased the concentration of the colloidal suspension while maintaining the same lift-up rate, the number of particles that assembled at the meniscus increased. This increase is due to the increase in the number of colloidal particles

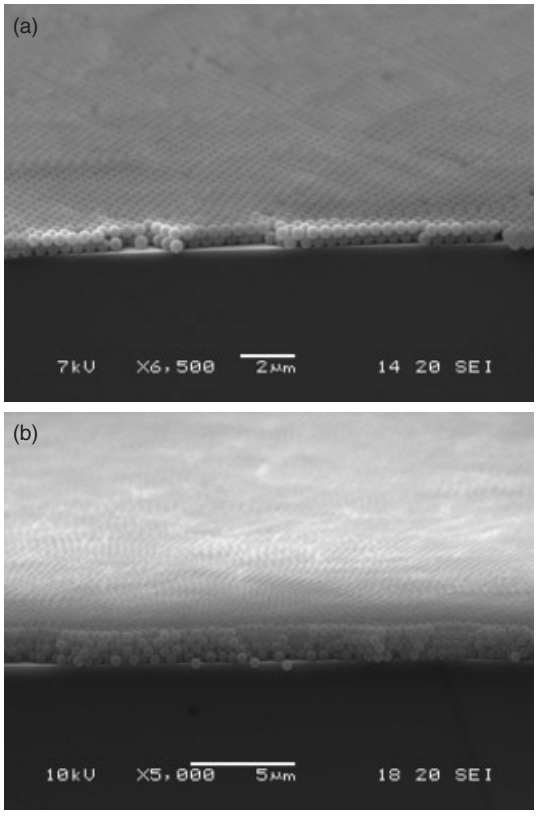

Figure 4. SEM side-view images of colloidal crystals with PS suspension concentrations of a) 1.0 wt.-% and b) 2.0 wt.-%.

that move towards the meniscus edge during the same period. Accordingly, multilayered colloidal crystals are formed. If we decreased the lift-up rate, we could fabricate thicker colloidal crystal film than the tetralayer. An example is given in the Supporting Information (Fig. S3).

On the basis of these experimental results, we plotted the number of layers against the inverse of the lift-up rate (Fig. 5a), the suspension concentration (Fig. 5b), and the appropriate lift-up rate for fabricating the monolayer against the suspension concentration (Fig. 5c). As shown in Figure 5, the thickness of the colloidal crystal increases as the lift-up rate decreases and the suspension concentration increases. Furthermore, the appropriate lift-up rate increases with increasing concentration.

Similar results have been observed for colloids deposited by a technique similar to ours on a glass plate. Dimitrov and Nagayama deposited a monolayer of colloids on smooth and wettable solid surfaces using the dipping apparatus.[2b] They derived a mathematical model to describe the growth rate of a 2D crystal array and extrapolated it for the growth of colloidal multilayers as follows[2b]

$$k = \frac{\beta L j_e \varphi}{0.605 v d (1-\varphi)} \quad (1)$$

where k is the number of layers, β is the ratio between the velocity of particles in the solution and the fluid velocity, L is the length of meniscus, j_e is the solvent evaporation rate, φ is the volume fraction of particles in the colloidal suspension, d is the diameter of the particles, and v is the withdrawal velocity of the substrate. [22] Our experimental data, which is shown in Figure 5, appears to agree well with the above equation.

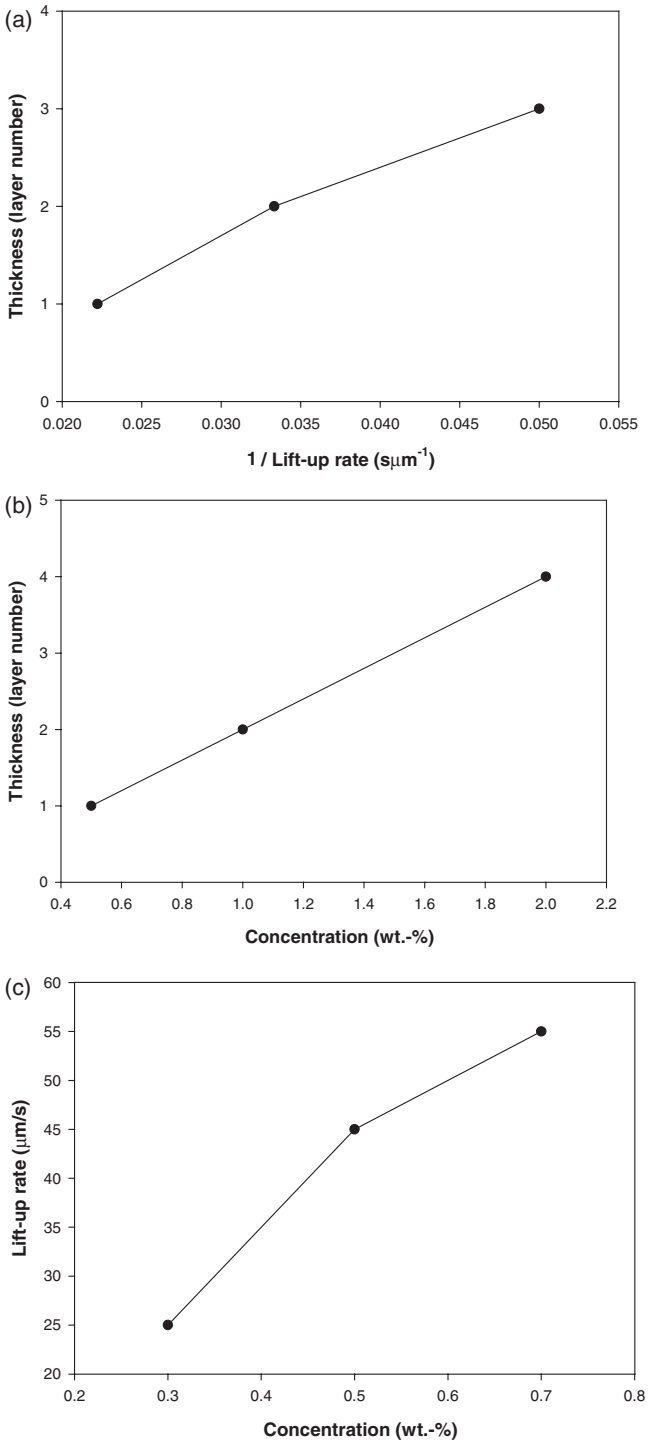

Figure 5. a) Dependence of the film thickness on the inverse of the lift-up rate at the same concentration (0.5 wt.-%). b) Dependence of the film thickness on the suspension concentration at the same lift-up rate (45 $\mu m\,s^{-1}$). c) The appropriate lift-up rate for fabricating monolayered colloidal crystals at different concentrations.

ADVANCED FUNCTIONAL MATERIALS

In addition to the lift-up rate and the suspension concentration, we investigated the effect of the evaporation rate of water. In our system, the evaporation rate of water can be controlled by blowing hot air. Initially, we carried out the experiment without blowing hot air. In the experiment, we used a 0.5 wt.-% PS colloidal suspension (PS colloid 460 nm in diameter), and we lifted the back glass substrate at a rate of 45 $\mu m\,s^{-1}$. When we blew hot air, the resulting colloidal crystal showed a well-ordered monolayer under the experimental condition. In Figure 6, which shows a surface SEM image of the sample, the colloidal particles assembled into sparse structures. Without blowing hot air, the water evaporation rate was slower. Hence, the colloidal particles assembled into sparse structures, because the number of particles that assembled at the meniscus was also smaller. We also had to increase the concentration of the colloidal suspension or decrease the lift-up rate in order to obtain well-ordered colloidal crystals. Therefore, the blowing of hot air is necessary to rapidly deposit 2D or 3D colloidal crystals using small quantities of PS colloidal suspension.

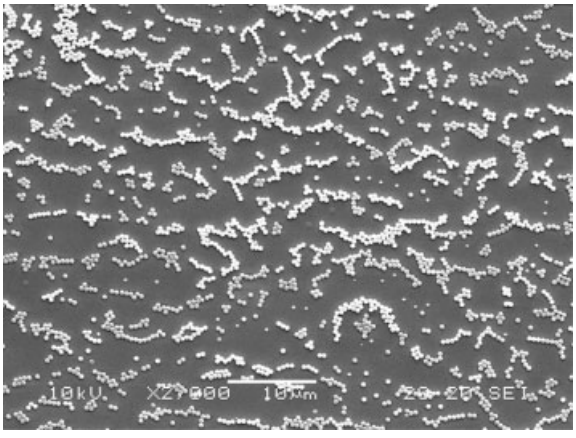

Figure 6. SEM surface image of colloidal particles assembled without blowing hot air.

One important criterion for the validity of an assembling method is whether the method can be applied to colloidal particles of various sizes. We therefore tried to fabricate monolayered colloidal crystals in a 0.5 wt.-% PS suspension with particle diameters of 600, 360, and 260 nm. Our expectation was that the optimal lift-up rate for assembling colloidal particles into highly ordered structures would vary with the size of the colloidal particles. We subsequently obtained monolayered colloidal crystals with 600, 360, and 260 nm PS colloidal particles by lifting the glass substrate at the rate of 40, 45, and 55 $\mu m\,s^{-1}$. Figure 7 shows the resulting SEM surface images for the 600, 360, and 260 nm PS colloidal particles. While these images reveal some point and line defects, the colloidal particles are ordered into monolayers over large areas. Therefore, we deduce that our new method can be applied to colloidal particles of various sizes. We believe that the number of defects can be reduced if we reduce the polydispersity of the colloidal particles.

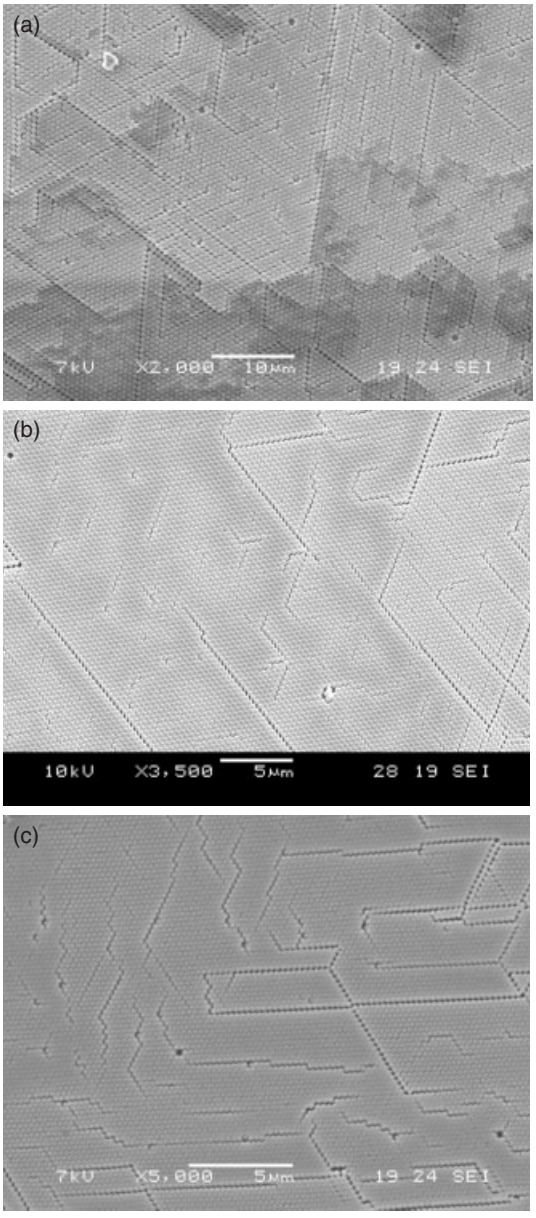

Figure 7. SEM surface images of the monolayered colloidal crystals fabricated with a) 600 nm, b) 360 nm, and c) 260 nm PS colloidal particles.

Finally, we applied our method to the fabrication of binary colloidal crystals, by consecutively depositing layers of large and small colloidal particles. First, we obtained monolayered colloidal crystals consisting of 460 nm PS colloidal particles as explained above. We then used the same process with the same lift-up rate (45 $\mu m\,s^{-1}$) to deposit 0.1 wt.-% 230 nm colloidal particles on the monolayer of colloidal crystals. Figure 8 shows the SEM surface image of the resulting binary colloidal crystals (the size ratio, $\gamma = R_S/R_L = 0.5$, where R_S is the radius of the smaller colloid and R_L the radius of the larger colloid). The small colloidal particles settled within the interstitial sites between the hexagonally close-packed large particles, thereby forming a graphite-structured lattice. As shown in Figure 8,

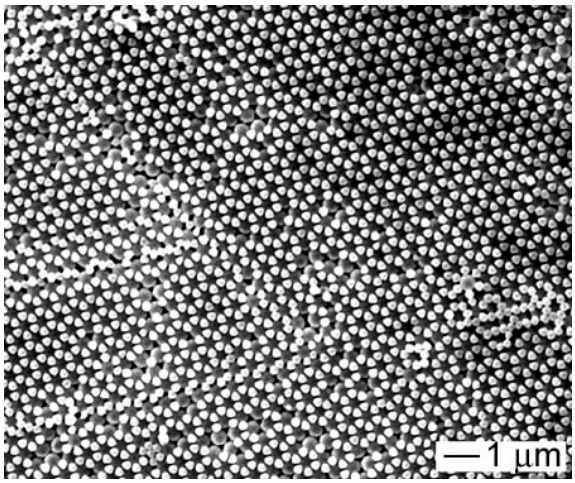

Figure 8. SEM surface image of the binary colloidal crystal consisting of 460 nm and 230 nm PS colloidal particles.

our system is useful for fabricating high-quality binary colloidal crystals. If we can properly adjust the volume fractions of the large and small colloidal spheres, and the ratio of the diameters of the small and large spheres, we can fabricate binary colloidal crystals with various structures.

3. Conclusion

We have used a confined convective assembly to fabricate 2D and 3D colloidal crystals. Water evaporation was used to assemble the colloidal particles into a mono- or multilayer at the meniscus edge. The lift-up rate of the back glass substrate affected the meniscus-thinning rate and thereby determined whether the colloidal particles assembled into 2D or 3D shapes. This method was valid for the fabrication of monolayered colloidal crystals with colloidal particles of various sizes (260 nm, 360 nm, 460 nm, and 600 nm). We also used this method to fabricate a multilayered colloidal crystal and binary colloidal crystals. These 2D and 3D colloidal crystals can be used as masks for photolithography, as master molds for 2D regular arrays, and as templates for 3D photonic bandgap crystals.

4. Experimental

Materials and Substrates: To prepare the 230 nm PS colloidal particles, we used emulsifier-free emulsion polymerization to synthesize submicrometer-sized PS particles [23]. We poured deionized water (450 g) into a reactor and kept the water at a temperature of 70 °C while stirring it at 350 rpm (rpm: revolutions per minute). We then added sodium styrene sulfonate (0.3 g) to the water as an emulsifier and sodium hydrogen carbonate (0.25 g) as a buffer. After 10 min, we added styrene monomer (50 g) to the solution. After 1 h, we added potassium persulfate (0.25 g) to the solution as an initiator. Finally, we performed polymerization under a nitrogen atmosphere for 18 h. To prepare the 260, 360, and 460 nm PS colloidal particles, we followed the same procedure except that we varied the content of sodium styrene sulfonate (0.25, 0.09, and 0.05 g, respectively). To prepare 600 nm PS colloidal particles, we used sodium methacrylate (0.02 g) instead of sodium hydrogen carbonate, and we increased the quantity of styrene monomer from 50 to 60 g. The concentration of obtained 600 nm PS colloidal particles was ca. 12 wt.-% and the concentration of the other particles was ca. 10 wt.-%. To fabricate the colloidal crystals films, we used deionized water as a dispersing solvent and we diluted the concentrations of the colloidal suspensions. Finally, we added a small amount of polyvinylpyrrolidone (weight fraction of polyvinylpyrrolidone, $\phi = 6.3 \times 10^{-4}$) to the suspension. The polyvinylpyrrolidone used in this study has an average weight-average molecular weight, M_w, of 55 000, and was purchased from Aldrich. The slide glasses (76 mm × 26 mm) were produced by Waldemar Knittel, Inc., Germany. The glass substrates were cleaned with ethanol and treated with oxygen plasma to make their surfaces hydrophilic.

Fabrication of Colloidal Crystal Films: A Photograph of the experimental set-up for confined convective assembly is shown in the Supporting Information (Fig. S1). We connected a back glass substrate to a dipping machine to control the lift-up rate and then attached a front glass substrate that was separated from the back glass substrate by a gap of approximately 100 μm. (We attached Scotch tape to both side edges of the back glass substrate; the tape plays the role of a spacer.) Using a micropipette, we inserted an aqueous suspension (about 100 μL) of colloidal particles into the gap between the two glass substrates. Finally, we raised the back glass substrate at the specific rates while blowing hot air towards the meniscus that formed at the interface of the glass substrate and the colloidal suspension.

Instrumentation: The dipping machine is an automation stage controlled by a controller, and its dipping speed can be varied over a range of 0.5 $\mu m\,s^{-1}$ to 500 $\mu m\,s^{-1}$. The dipping machine and controller are products of Sigma Koki Co., Japan. The SEM images of the colloidal crystals films were obtained using a JSM 5610, JEOL Co. The samples for SEM measurements were placed on carbon surfaces and then coated with Au.

Received: December 22, 2005
Final version: March 28, 2005

[1] a) U. C. Fisher, P. Zingsheim, *J. Vac. Sci. Technol.* **1981**, *19*, 881. b) C. L. Haynes, R. P. Van Duyne, *J. Phys. Chem. B* **2001**, *105*, 5599.

[2] a) N. D. Denkov, O. D. Velv, P. A. Kralchevsky, I. B. Ivanov, H. Yoshimura, K. Nagayama, *Langmuir* **1992**, *8*, 3183. b) A. S. Dimitrov, K. Nagayama, *Langmuir* **1996**, *12*, 1303. c) A. S. Dimitrov, T. Miwa, K. Nagayama, *Langmuir* **1999**, *15*, 5257.

[3] a) B. Van Duffel, R. H. A. Ras, F. C. De Schryver, R. A. Schoonheydt, *J. Mater. Chem.* **2001**, *11*, 3333. b) M. Szekeres, O. Kamalin, R. A. Schoonheydt, K. Wostyn, K. Clays, A. Persoons, I. Dekany, *J. Mater. Chem.* **2002**, *12*, 3268. c) S. Reculusa, S. Ravaine, *Chem. Mater.* **2003**, *15*, 598.

[4] a) M. Trau, D. A. Saville, I. A. Aksay, *Science* **1996**, *272*, 706. b) M. Trau, D. A. Saville, I. A. Aksay, *Langmuir* **1997**, *13*, 6058.

[5] a) F. Burmeister, C. Schafle, B. Keilhofer, C. Bechinger, J. Boneber, P. Leiderer, *Adv. Mater.* **1998**, *10*, 495. b) C. L. Haynes, R. P. Van Duyne, *J. Phys. Chem. B* **2001**, *105*, 5599. c) J. C. Hulteen, R. P. Van Duyne, *J. Vac. Sci. Technol. A* **1995**, *13*, 1553.

[6] a) D. Wang, H. Möhwald, *Adv. Mater.* **2004**, *16*, 244. b) R. E. Schaak, R. E. Cable, B. M. Leonard, B. C. Norris, *Langmuir* **2004**, *20*, 7293.

[7] a) S. John, *Phys. Rev. Lett.* **1987**, *58*, 2486. b) Z. Y. Li, J. Wang, B. Y. Gu, *Phys. Rev. B* **1998**, *58*, 3721. c) Y. Xia, B. Gates, X.-Y. Li, *Adv. Mater.* **2001**, *13*, 409.

[8] a) O. D. Velev, P. M. Tessier, A. M. Lenhoff, E. W. Kaler, *Nature* **1999**, *401*, 548. b) D. J. Norris, Y. A. Vlasov, *Adv. Mater.* **2001**, *13*, 371. c) I. Soten, H. Miguez, S. M. Yang, S. Petrov, N. Coombs, N. Tetreault, N. Matsuura, H. E. Ruda, G. A. Ozin, *Adv. Funct. Mater.* **2002**, *12*, 71. d) F. Yan, W. A. Goedel, *Adv. Mater.* **2004**, *16*, 911.

[9] a) W. Lee, S. A. Pruzinsky, P. V. Braun, *Adv. Mater.* **2002**, *14*, 271. b) T. A. Taton, D. J. Norris, *Nature* **2002**, *416*, 685.

[10] P. Tran, *J. Opt. Soc. Am. B* **1997**, *14*, 2589.

ADVANCED FUNCTIONAL MATERIALS

[11] a) J. M. Weissman, H. B. Sunkara, A. S. Tse, S. A. Asher, *Science* **1996**, *274*, 959. b) S. H. Park, Y. Xia, *Langmuir* **1999**, *15*, 266.
[12] a) K. Lee, S. A. Asher, *J. Am. Chem. Soc.* **2000**, *122*, 9534. b) Y.-J. Lee, P. V. Braun, *Adv. Mater.* **2003**, *15*, 563.
[13] H. Miguez, F. Meseguer, C. Lopez, A. Blanco, J. S. Moya, J. Requena, A. Mifsud, V. Fornes, *Adv. Mater.* **1998**, *10*, 480.
[14] a) P. Jiang, J. F. Bertone, K. S. Hwang, V. L. Colvin, *Chem. Mater.* **1999**, *11*, 2132. b) Y. H. Ye, F. Leblanc, A. Hache, V. V. Truong, *Appl. Phys. Lett.* **2001**, *78*, 52. c) L. M. Goldenberg, J. Wagner, J. Stumpe, B.-R. Paulke, E. Gornitz, *Langmuir* **2002**, *18*, 3319.
[15] Y. A. Vlasov, X.-Z. Bo, J. C. Sturm, D. J. Norris, *Nature* **2001**, *414*, 289.
[16] a) M. Holgado, F. Garcia-Santamaria, A. Blanco, M. Ibisate, A. Cintas, H. Miguez, C. J. Serna, C. Molpeceres, J. Requena, A. Mifsud, F. Meseguer, C. Lopez, *Langmuir* **1999**, *15*, 4701. b) A. Rogach, N. A. Kotov, D. S. Koktysh, J. W. Ostrander, G. A. Ragoisha, *Chem. Mater.* **2000**, *12*, 2721.
[17] a) S. H. Im, Y. T. Lim, D. J. Suh, O O. Park, *Adv. Mater.* **2002**, *14*, 1367. b) S. H. Im, O O. Park, *Langmuir* **2002**, *18*, 9642.
[18] S. Wong, V. Kitaev, G. A. Ozin, *J. Am. Chem. Soc.* **2003**, *125*, 15 589.
[19] K. P. Velikov, C. G. Christova, R. P. A. Dullens, A. van Blaaderen, *Science* **2002**, *296*, 106.
[20] a) R. D. Deegan, D. Bakajin, T. F. Dupont, G. Huber, S. R. Nagel, T. A. Witten, *Nature* **1997**, *389*, 827. b) R. D. Deegan, *Phys. Rev. E* **2000**, *61*, 475. c) L. Shmuylovich, A. Q. Ahen, H. A. Stone, *Langmuir* **2002**, *18*, 3441.
[21] S. H. Im, M. H. Kim, O O. Park, *Chem. Mater.* **2003**, *15*, 1797.
[22] C.-A. Fustin, G. Galsser, H. W. Spiess, U. Jonas, *Langmuir* **2004**, *20*, 9114.
[23] a) J. H. Kim, M. Chainey, M. S. El-Aasser, J. W. Vanderhoff, *J. Polym. Sci., Part A: Polym. Chem.* **1992**, *30*, 171. b) G. R. Yi, J. H. Moon, S.-M. Yang, *Chem. Mater.* **2001**, *13*, 2613.

